한국형 WA-DGNSS를 위한 WAAS 대류층 지연 보정모델의 성능연구

Performance Test of the WAAS Tropospheric Delay Model for the Korean WA-DGNSS

안용원*, 김동현*, Jason Bond**, 최완식***

Yong-Won Ahn, Dong-Hyun Kim*, Jason Bond** and Wan-Sik Choi***

요 약

한반도 지역의 GNSS 관측소의 자료들을 처리하여 가강수량을 추정하였고, 그 결과를 기상 관측 장비인 radiosonde의 추정치와 비교하였다. 실험 조건을 일반화하기 위하여, 데이터는 일반적인 기상 조건과 악화되는 기상 조건을 이용하였다. GNSS의 자료들에서 처리한 결과들은 연구에서 이용한 고 해상도의 기상 관측 장비의 예측 값들과 대부분10 mm내외에서 서로 일치하였다. 따라서GNSS가 고해상도 기상 대체 장비라는 가정하에서, 현재 WAAS 대류층 지연 모델로 쓰이고 있는 UNB3 모델이 한반도 내에서 적절한 모델로 쓰일 수 있는지에 대한 적용 가능성에 대한 실험을 수행하였다. 빠르게 변화하는 총 습윤 지연 값에 대한 결과를 비교한 결과, UNB3의 대류층 지연 모델은 한반도와 같은 습한 지역 내에서는 보정 모델로 부적절하다는 예측 결과를 보였다. 결과적으로, 향후 한국형 SBAS인 WA-DGNSS의 경우, 대류층 지연 영향을 최소화하여 고정밀 vertical 항행 해를 얻기 위해서는 현재 WAAS에서 쓰이는 기존 대류층 모델을 직접 이용하기 보다는 향후 한반도의 기상 상황에 적절히 대처할 수 있는 새로운 대류층 지연 모델이나 GNSS 관측치 또는 기상수치모델을 이용한 준 실시간 모델이 적절할 것으로 조사되었다.

Abstract

The precipitable water vapor (PW) was estimated using Global Navigation Satellite System (GNSS) from several GNSS stations within the Korean Peninsula. Nearby radiosonde sites covering the GNSS stations were used for the comparison and validation of test results. GNSS data recorded under typical and severe weather conditions were used to generalize our approach. Based on the analysis, we have confirmed that the derived PW values from the GNSS observables were well agreed on the estimates from the radiosonde observables within 10 mm level. Assuming that the GNSS observables could be a good weather monitoring tool, we further tested the performance of the current WAAS tropospheric delay model, UNB3, in the Korean Peninsula. Especially, the wet zenith delays estimated from the GNSS observables and from UNB3 delay model were compared. Test results showed that the modelled approach for the troposphere (i.e., UNB3) did not perform well especially under the wet weather conditions in the Korean Peninsula. It was suggested that a new model or a near real-time model (e.g., based on regional model from GNSS or numerical weather model) would be highly desirable for the Korean WA-DGNSS to minimize the effects of the tropospheric delay and hence to achieve high precision vertical navigation solutions.

Key Words: UNB3, Tropospheric Delay(대류층 지연 보정), GNSS(위성항법시스템), WA-DGNSS (광역보정), WAAS(광역확대오차보정시스템)

I. INTRODUCTION

Three Satellite-Based Augmentation Systems (SBAS) are currently operational: Wide Area

* GPS Research Laboratory, Geodesy and Geomatics Engineering, University of New Brunswick.
** Gemini Navsoft Technologies Inc., Fredericton, New Brunswick, Canada.
*** ETRI (Electronics and Telecommunications Research Institute).
· 제1저자 (First Author): 안용원
· 투고일자 : 2011년 8월 7일
· 심사(수정)일자 : 2011년 8월 7일 (수정일자 : 2011년 8월 23일)
· 게재일자 : 2011년 8월 30일

Augmentation System (WAAS) from US, the European Geostationary Navigation Overlay System (EGNOS) from EU, and MTSAT Satellite Augmentation System (MSAS) from Japan. Other SBAS includes the GPS-Aided and GEO-Augmented Navigation System (GAGAN) from India and the Russian System of Differential Correction and Monitoring (SDCM) is currently in an early stage of development. The Ministry of Land, Transport and Maritime Affairs of the Korean government has their plan to develop a regional SBAS, called Wide-Area Differential GNSS (WA-DGNSS), due to its substantial advantages in the Korean Peninsula.

Each SBAS system uses its own broadcasting satellite system to distribute the correction information to the intended users. The fundamental observations on ground, however, are from GNSS. The received signals from GNSS satellites experience many different error sources. SBAS can reduce the ionospheric delay and orbital error significantly. The tropospheric delay, which mostly contributes to the height component of the station's coordinate estimates, is one of the largest limiting factors for high accuracy GNSS positioning. In addition to the SBAS, ground based augmentation system (GBAS) also addresses the importance of the troposphere to achieve reliable decorrelation parameter for mitigating the delay [1].

Typically, the tropospheric delay can reach up to 2.5 m in the zenith direction. It can be separated into two components; hydrostatic (dry) and non-hydrostatic (wet) component. The dry component which consists of 90% of total delay is stable and well predictable, whereas the wet component is highly variable. Assuming hydrostatic equilibrium, the dry component is well predicted whenever the surface pressure is known. Then the estimated dry component can be subtracted from the total delay to get the wet component. The wet component varies from a few mm level at the poles to up to 40 mm in the zenith direction in the tropics, and changes significantly in the direction of a weather front.

The troposphere is non-dispersive medium which does not depend on the current GNSS frequency ranges [2]. Multiple-frequency signals are not much helpful in mitigating the tropospheric delay although they may improve troposphere modeling by removing all frequency dependent errors in the observations. The most challenging problem is that the tropospheric parameters are highly correlated with the height component and hence any error of the troposphere is propagated into the height component to be estimated. For this reason, there is a strong demand for improving the techniques to mitigate the tropospheric delay and subsequently to improve the safety of SBAS users.

As UNB3 is based on average climatological behaviour in North America, the deterioration of positioning solutions is unavoidable once it is used in the Korean Peninsula. Especially during anomalous or humid weather conditions, the model will not be performed well. As a matter fact, UNB3 uses U.S. Standard Atmosphere parameter values of 1013.25 millibars (total pressure), 288.15 Kelvin's (temperature), 11.7 millibar (water-vapour pressure), 6.5 Kelvin's per kilometer (temperature lapse rate), and 3 (lambda parameter).

To have readers understand the troposphere model in Chapter II, the brief but fundamental principle of GNSS signal delays for the neutral atmosphere is presented herein. The neutral atmosphere can be divided into the troposphere, the tropopause and the stratosphere. The tropospheric delay of GNSS signals depends on the index of refraction n along the signal path which can be expressed in term of the refractivity N.

Especially, the refractivity of humid air in the frequency band between 100 MHz and 20 GHz is given as [3]:

$$N = k_1 \frac{p_d}{T} Z_d^{-1} + k_2 \frac{e}{T} Z_w^{-1} + k_3 \frac{e}{T^2} Z_w^{-1} \qquad (1)$$

where

p_d : partial pressure of dry air (mbar); $p_d = p - e$ with p being the total pressure

e : partial pressure of water vapor (mbar)

T : temperature (K)

k_1, k_2, k_3 : refraction constants ($K/mbar$, $K/mbar$, $K/mbar^2$)

Z_d^{-1} , Z_w^{-1} : inverse compressibility factors for dry and wet air which are empirical factors

The first term on right hand side in Eq. (1) is the hydrostatic component and represents the effect of the induced dipole moment of the dry component. The second term is related to the dipole moment of water vapor and the last term represents the dipole orientation effects of the permanent dipole moment of water vapor molecules. The last two terms in Eq. (1) constitutes the wet component of the refractivity. The refraction constants $(k_1, k_2 \text{ and } k_3)$ are determined empirically. The inverse compressibility accounts for the difference between ideal gas assumptions and non-ideal gas behavior. These values and the pressure of water vapor are given in [3][4][5].

In order to define the zenith delay, it is necessary to express the refractivity in Eq. (1) in terms of its hydrostatic and wet components. Based on the assumption of the hydrostatic equilibrium, the refractivity can be strictly separated between the hydrostatic and wet components. Detailed derivation can be found on [4], where the hydrostatic and non-hydrostatic components are given as:

$$N_d = k_1 \frac{\rho R_o}{M_d'} \qquad N_w = \left(k_2' \frac{e}{T} + k_3 \frac{e}{T^2} \right) Z_w^{-1} \quad (2)$$

where

$$k_2' = \left(k_2 - k_1 \frac{M_w}{M_d} \right)$$

R_o : universal gas constant ($J\,mol^{-1}\,K^{-1}$)

M_w : molar weight of wet air ($kg\,kmol^{-1}$)

M_d : molar weight of dry air ($kg\,kmol^{-1}$)

$$k_1 = 77.6 \pm 0.05 K/hPa$$

$$k_2 = 70.4 \pm 2.2 K/hPa$$

$$k_3 = (3.739 \pm 0.02) \cdot 10^5 K^2/hPa$$

Finally, the zenith hydrostatic delay and the zenith wet delay can be defined as follows:

$$ZHD = 10^{-6} \int_{h_s}^{\infty} N_d \, dh, \qquad ZWD = 10^{-6} \int_{h_s}^{\infty} N_w dh \quad (3)$$

where

h_s : surface height

dh : differential increment in height

The hydrostatic delay can be easily modeled by the assumption of hydrostatic equilibrium with an accuracy of the millimetre level [6]. However, unlike the hydrostatic part, the wet part, which amounts to approximately 10-40 cm of range delay, is much more difficult to model than the hydrostatic part due to its strong spatial and temporal variations. The assumption of hydrostatic equilibrium does not hold for this portion of the air and relative errors of empirical/theoretical models are on the order of 10%. This uncertainty in modeling (which leaves large residual errors) can cause significant errors in high-precision GNSS applications. Since these variations can generate relative and absolute tropospheric errors, the error in the estimation of tropospheric corrections for one station with respect to another in a network can cause relative tropospheric errors, which mostly results in incorrect estimates of station's height coordinates.

II. Tropospheric Delay Models

2-1 Ray-Tracing using NWP (RUC20)

When both GNSS and 3-D numerical weather fields are available, the path of a satellite signal can be calculated by using a ray-tracing technique. This will give more reliable estimates of the tropospheric delay for low elevation angles. Ray-tracing is known as one of the most reliable and realistic approaches for calculating the tropospheric delay [7]. To maximize its usage, tropospheric delays for all incoming signals from a given satellite should be respectively calculated in real-time for the given sampling rate. This would take much more time than using the mathematical models. Direct application of the ray-tracer, using 3-D numerical weather fields, to GNSS real-time applications has some limitations due to the reason. Figure 1 briefly illustrates a ray-tracing technique based on the Snell's law used in this study.

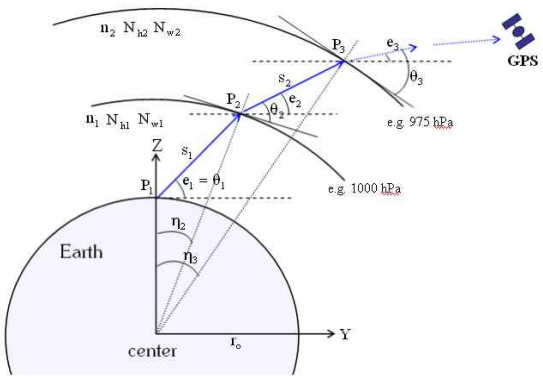

Fig. 1. A ray-tracing scheme [8]
그림 1. Ray-tracing 도해

At the top k (~ up to 1000) level, the hydrostatic and wet refractivity can be calculated. Then the refractivity index of the dry and wet component and between the k and k-1 level can be estimated.

Using the following relationship between the height of the levels and the distance to the center of the Earth, the corresponding distance is calculated as:

$$r_i = r_o + h_i \tag{4}$$

where subscript i represents the corresponding level.

When the initial angle is given, the point P_1 can be determined by using the relation, $\theta_1 = e_1$. After this calculation, the second point P_2 and geocentric coordinates of P_1 and P_2 can be determined as [7]:

$$\begin{aligned} s_1 &= -r_1 \sin\theta_1 + \sqrt{r_2^2 - r_1^2 \cos^2\theta_1} \\ z_1 &= r_1 \qquad\qquad y_1 = 0 \\ z_2 &= z_1 + s_1 \sin e_1 \qquad y_2 = y_1 + s_1 \cos e_1 \end{aligned} \tag{5}$$

The corresponding angles at the center of the Earth can be determined as:

$$\eta_1 = 0, \qquad \eta_2 = \arctan(y_2 / z_2) \tag{6}$$

Now, the angles θ_2 and e_2 at the point P_2 can be determined based on the Snell's law as:

$$e_2 = \theta_2 - \eta_2, \quad \theta_2 = \arccos\left(\frac{n_1}{n_2}\cos(\theta_1 + \eta_2)\right) \tag{7}$$

The same procedures are applied to integrate all other shells from 2 to (k-1) levels. Then, one can estimate the hydrostatic slant delay ds_h and the wet slant delays ds_w using the discrete ray-tracing technique as follows:

$$ds_h = \sum_{i=1}^{k-1} s_i N_{h_i} \qquad ds_w = \sum_{i=1}^{k-1} s_i N_{w_i} \tag{8}$$

The GPS-Met Observing Systems Branch (GPS-Met) within the Forecast Systems Laboratory (FSL) in the

National Oceanic and Atmospheric Administration (NOAA) use Rapid Update Cycle, called RUC. RUC20 data used in this study has a horizontal grid of 301 by 225 points, and is based on a 20 x 20 km grid. It has 37 isobaric levels (with an additional ground surface level) as a three-dimensional gridded field from 1000 hPa to 100 hPa, at intervals of 25 hPa. It also has 92 variables which contain necessary information for calculating refractivity (e.g., geopotential height, relative humidity, pressure, temperature, etc.).

Using RUC20, temperature T,total pressure P,andspecifichumidityareinterpolated.Thepartialpressurefo rdrygasesiscomputedby $P_d = P - e$ where e(mbar)denotespartialpressureofwatervapor.

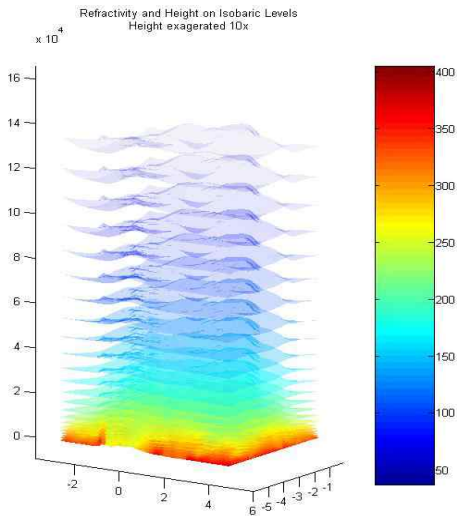

Fig. 2. Refractivity calculated for each layer from RUC20 raw data
그림 2. RUC20 수치모델을 이용한 각 레이어의 굴절률 값

The refractivity N at a given distance ℓ along the path is obtained by interpolating the weather parameters at the corresponding three-dimensional position in the NWP gridded fields. Nissampledatasmanypointsasneededtofulfillthetolerancere quirement(e.g.,1mm).Atypicalcurveofrefractivityversusdis tancefromthereceivertowardsthesatellite(with1mmtoleranc e)canbefoundin[9].Figure 2 illustrates the refractivity profile calculated for each layer from RUC20 raw data. Each level contains refractivity index and isobaric height covering the whole North America, and lower Canada, and upper Mexico region. Figure 5 in section III was derived based on this layered refractivity profile. Each node spacing 20 km apart from nearby nodes has detailed meteorological parameters, and they were used for the delay calculations for a specific GPS satellite in view.

2-2 Ray-Tracing using Radiosonde

Radiosonde is a balloon-borne instrument with radio transmitting capabilities. Typically, weather offices launch balloons twice each day at the same time to obtain basic weather information about the atmosphere. The instruments carried by the balloon measure different weather parameters such as air temperature, humidity and pressure with height (typically to altitudes of approximately 30 km), and their data are transmitted immediately to the ground station by a radio transmitter. Radiosonde observations, also called RAOB, has been the main source of upper air measurements for over 70 years and still seems to be an important source of data for neutral-atmosphere studies. RAOB data in a ray tracing service can still be an option for research and validation studies. Figure 3 shows the location of RAOB launch sites (~1000 sites worldwide), whose data are accessible through the National Oceanic and Atmospheric Administration (NOAA) database.

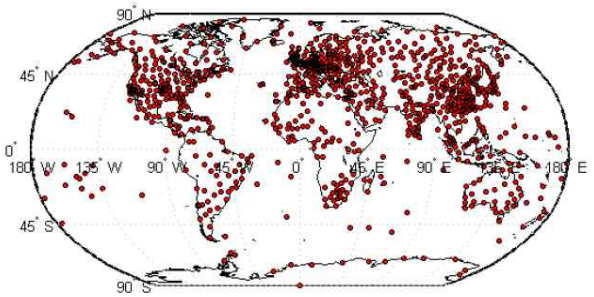

Fig. 3. RAOB sites around the world [10]
그림 3. 전 세계의 라디오존데 관측소 현황

Typically, ray-tracing is performed using radiosonde data to generate an absolute or true value for validating

the zenith wet delay. Although radiosonde provides a good vertical resolution, they are not typically used due to their poor horizontal resolution and cost. Here is the methodology to derive the PW from RAOB for this test.

If we know dew point and temperature on certain elevation, we can get the relative humidity based on the Clausius-Clapeyron equation:

$$T - T_d = 4.25 \times 10^{-4} \cdot T \cdot T_d \cdot (-\log U_w) \quad (9)$$

where,

T : temperature (K),

T_d : dew point temperature (K),

U_w : relative humidity (%),

Based on the Magnus's formula, saturated water vapor pressure can be calculated as:

$$\log e_w = \frac{-2973.4}{T} - 4.9283 \cdot \log T + 23.5470 \quad (10)$$

where e_w is saturated water vapor pressure.

Integrated Water Vapor (IWV) gives the total amount of water vapor that a signal from the zenith direction would encounter. Precipitable Water Vapor (PWV) is the IWV scaled by the density of water. IWV can be formulated as follows:

$$IWV = \int_0^H \rho_w dh = \int_0^H \rho q dh \quad (11)$$

where,

ρ : density, and $q = r/(1+r)$

The mixing ratio (r)canbewrittenasfollows:

$$r = \frac{U_w r_w}{1 + \frac{(1-U_w) r_w}{\varepsilon}} \quad (12)$$

where,

$r_w = \varepsilon \cdot e_w / (P - e_w)$

ε : constant

As $-dP = \rho g dh$, IWV becomes

$$IWV = \frac{1}{g} \int_{P_o}^{P_H} q dP \quad (13)$$

where,

g : gravitational constant on Earth surface

P_o, P_H : pressure where $h = 0, h = H$

In the discrete case, IWV can be specifically summarized as follows [11]:

$$IWV = 0.0102 \sum_{k=1}^{N} \overline{q}_k \Delta P_k \quad (14)$$

where,

$$\overline{q}_k = \frac{q_k + q_{k-1}}{2}, \ \Delta P_k = P_k - P_{k-1}$$

Therefore, precipitable water vapour (PW) can be calculated based on the following formula.

$$PW = \frac{IWV}{\rho_w} \quad (15)$$

Zenith wet delay (ZWD) using GPS data can be calculated from the relationship, ZWD=ZTD−ZHD, where ZTD represents the zenith total delay. The total delay can be estimated from GPS data. When the surface pressure, height, and latitude are known, the hydrostatic component can be determined using Saastamoinen hydrostatic delay model [12]. Equation (2) can be rewritten using the mean gravity acceleration as:

$$N_d = k_1 \frac{\rho R_o}{M_d} = k_1 R_d \rho = -k_1 R_d \frac{1}{g_m} \frac{dp}{dH}. \quad (16)$$

Substituting Eq. (16) into Eq. (3) gives

$$ZHD = 10^{-6}\int_{H_s}^{\infty} N_d dH = -10^{-6} k_1 R_d \frac{1}{g_m}\int_{p_s}^{\infty} dp = -10^{-6} k_1 R_d \frac{p_o}{g_m}. \quad (17)$$

where g_m is the weighted mean gravity acceleration.

The weighted mean gravitational acceleration at the center of mass of the vertical atmospheric column directly above the station can be approximated by the Saastamoinen equation [13] as:

$$g_m = 9.784 \cdot (1 - 0.00266\cos 2\varphi - 0.00028H) = 9.784 \cdot f(\varphi, H), \quad (18)$$

where φ and H (km) are the latitude and height of the station, respectively. Therefore, the ZHD becomes:

$$ZHD = \frac{0.0022767\, p_o}{1 - 0.00266\cos 2\varphi - 0.00028H}. \quad (19)$$

The troposphere can be expanded to further distinguish between the azimuthally symmetric delay and asymmetric parts 4]. The asymmetric components can be determined using a horizontal tropospheric gradient model. One way to deal with this is a 'tilting' technique [14]. Once the ZWD is estimated, the PW can be calculated by [4]:

$$Q = \frac{ZWD}{PW} = 0.10200 + \frac{1708.08\left(^{o}\mathrm{K}\right)}{T_m}, \quad (20)$$

$$T_m = 70.29\left(^{o}\mathrm{K}\right) + 0.72T_0\left(^{o}\mathrm{K}\right), \quad (21)$$

where,

T_m : mean temperature of the atmosphere (K),

T_0 : surface temperature (K).

In order to retrieve the PW, the mean temperature is necessary. We used the empirical values of in Eq. (21) as the mean value for Korea Peninsula was not available for analysis. The derived PW was compared with that of the observed radiosonde for this test.

2-2 UNB3 Tropospheric Delay Model

The UNB3 model for neutral atmosphere signal propagation delay is a hybrid model consisting of the Saastamoinen vertical propagation delay models, the Niell mapping functions, a look-up table of surface meteorological parameter values, and models to propagate these surface values to any arbitrary station height. The model was derived, in part, from the 1966 U.S. Standard Atmosphere Supplements. It was validated by comparing to ray-traced radiosonde measurements of the signal delay obtained from 173 stations in North America between 1987 and 1996. The model input parameters are day-of-year, elevation angle, height and latitude. The UNB3 model was originally developed by the University of New Brunswick (UNB) for the FAA-WAAS program. For the WAAS receiver firmware model, the Niell mapping functions have been used [15].

The temperature and humidity profiles contained in the 1966 U.S. Standard Atmosphere Supplements were used to derive values for the five meteorological parameters. As the primary driving parameters of the tropospheric delay it is natural that we choose total pressure P_o, temperature T_o and water vapour pressure e_o at the surface. The vertical profile of these parameters can be specified through the temperature lapse rate β and a parameter that represents the average decrease of water vapour λ [16].

For each latitude in the standard, the mean and the amplitude of the five parameters were calculated from

the January and June profiles. Between latitudes, linear interpolation is applied so that for a required parameter x at latitude f and time t [15]:

$$\xi(\phi,t) = \xi_{avg}(\phi_i) + \left[\xi_{avg}(\phi_{i+1}) - \xi_{avg}(\phi_i)\right]\cdot m - \left(\xi_{amp}(\phi_i) + \left[\xi_{amp}(\phi_{i+1}) - \xi_{amp}(\phi_i)\right]\cdot m\right)\cdot \cos\left(\frac{2\pi(t-28)}{265.25}\right) \quad (22)$$

where $m = (\phi - \phi_i)/(\phi_{i+1} - \phi_i)$.

The subscripts refer to the nearest latitudes specified in the table to the required one

For consistency with the Niell functions, day-of year 28 is used for the phase of the temporal variation. This model is described in Table 1 and is designated UNB3.

Table 1. Parameters for UNB3 model [15]
표 1. UNB3 모델의 각 변수 값들

Mean	P_o	T_o	e_o	β	λ
15	1013.25	299.65	26.31	6.30	2.77
30	1017.25	294.15	21.79	6.05	3.15
45	1015.75	283.15	11.66	5.58	2.57
60	1011.75	272.15	6.78	5.39	1.81
75	1013.00	263.65	4.11	4.53	1.55
Amp.	P_o	T_o	e_o	β	λ
15	0.00	0.00	0.00	0.00	0.00
30	-3.75	7.00	8.85	0.25	0.33
45	-2.25	11.00	7.24	0.32	0.46
60	-1.75	15.00	5.36	0.81	0.74
75	-0.50	14.50	3.39	0.62	0.30

Ⅲ. TEST RESULTS

As the UNB3 tropospheric model is widely used for SBAS application, several comparisons were mainly conducted to evaluate the performance of UNB3.

3-1 Non-Hydrostatic Delay Comparison between UNB3 and NWP (NOAA RUC20)

Weather fronts, temperature inversions, and other dynamic coastal weather phenomena can degrade the effectiveness of generic tropospheric delay models. UNB and the University of Southern Mississippi have collaborated to conduct a long-term experiment in precise GPS positioning over long distances in a marine environment. A pair of GPS reference stations on either side of the Bay of Fundy, Saint John (CGSJ) and Digby (DRHS), and on the ferry, as a part of the Princess of Acadia project, in Eastern Canada, has been deployed with NovAtel's DL-4 geodetic receivers and GPS-600 antennas. Kinematic GPS data from all three GPS receivers, meteorological stations and tide gauges were collected for a period of over one year (from November 2004 to December 2004). Figure 4 shows the geographic location of the project. The ferry traveled the same routes at the terminals of an approximately 76 km ferry route of two to four times daily, depending upon the season. The Bay of Fundy is located in a temperate climate with significant seasonal tropospheric variations (e.g., temperatures between − 30°C and + 30°C) [9]. As there is no numerical model available in Korea, this area and data had been specifically chosen to simulate the similar humid environment like Korea.

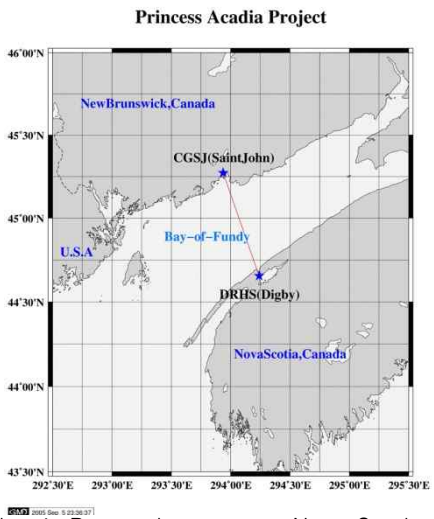

Fig. 4. Boat trajectory near Nova Scotia
그림 4. 캐나다 노바스코샤 주 근처의 선박 운행로

For the test, NOAA's RUC20 NWP model was used to calculate each total slant delay for all satellites in

view. At the same time, the total slant delay was obtained from UNB3 for the comparison. Figure 5 shows their comparison results.

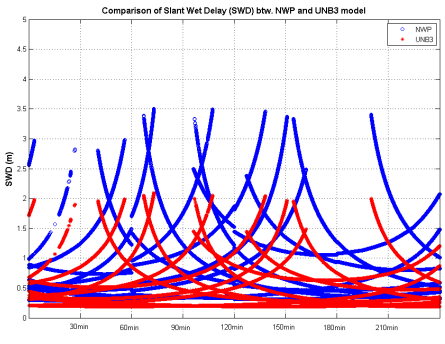

Fig. 5. Slant wet delay for GPS satellites based on NWP (RUC20) and UNB3 model
그림 5. 수치모델인 RUC20와 UNB3모델로 계산된 GPS위성들의 사선 방향의 습윤 지연량

As expected, there were substantial differences between two approaches. At lower elevation angles, the difference reached over 1 meter. This can potentially deteriorate entire navigation solution due to the wrongly fixed ambiguity parameters on the GPS processing.

3-2 PW Estimates using GPS Observations and Radiosonde (RAOB)

To evaluate the GPS-derived tropospheric delay, radiosonde data were processed to calculate PW. We analyzed the data during a severe weather event. Figure 6 presents a GMS infrared satellite image capturing a typhoon, RUSA, passing over the Korean Peninsula during summer in 2002. The typhoon was one of the worst in Korean meteorological history as it took 184 lives and destroyed 9900 buildings. The data used for this test were recorded at five permanent GPS stations controlled by Korea Astronomy and Space Science Institute (KASI) from August 25th to September 2nd. To get the best possible absolute ZTDs, and to decorrelate the zenith delay and height component, one distant station TSKB in Japan was incorporated into the data analysis.

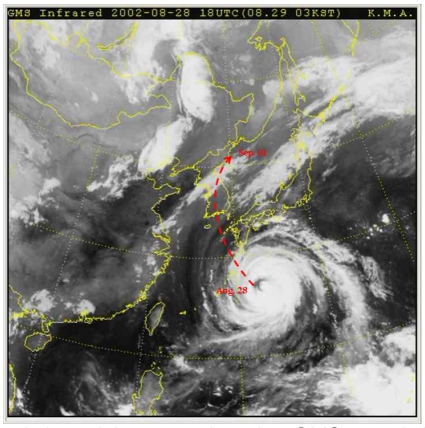

Fig. 6. Infrared image taken by GMS at 18 UTC on 28 August 2002 [17]
그림 6. 2002년 8월 28일 UTC 18시 GMS위성으로 촬영된 적외선 이미지

The detailed track of the typhoon during its passage in Korea Peninsula, and the figure for the GPS sites and radiosonde sites used for this research can be found on [18]. We processed the radiosonde data to compare the PW estimates driven by GPS. Station coordinates are summarized in Table 2.

Table 2: Station coordinates involved
표 2. 이용된 국내 GPS 관측소의 위치

ID	Lat.(deg.)	Long.(deg.)	Hgt.(m)
MKPO	34.8167	126.367	64.4074
SKCH	38.25	128.55	46.0738
SKMA	37.4833	126.917	61.7199
DAEJ	36.3833	127.367	116.848
JEJU	33.2833	126.45	430.226

To process GPS data, Bernese software was used. Once all of the station networks were formed and cycle slips were detected and repaired, the L1 and L2 ambiguities were resolved using a stochastic ionosphere approach (namely, the quasi-ionosphere approach). After all possible ambiguities were resolved, these fixed ambiguities were introduced to form ionosphere-free combination and to get the final positioning solutions. Subsequently, tropospheric parameters were estimated. During Bernese data processing, IGS final SP3 orbit products were used. For the comparison, the RAOB data, pressure, precipitation, and other meteorological

data recorded from the Korea Meteorological Administration (KMA) were used. Figure 7 illustrates the pressure curve recorded on KMA.

From the pressure curve, it is evident that the typhoon passed the Korean Peninsula during August 31standSeptember1st. During the passage of the typhoon, torrential rain occurred.

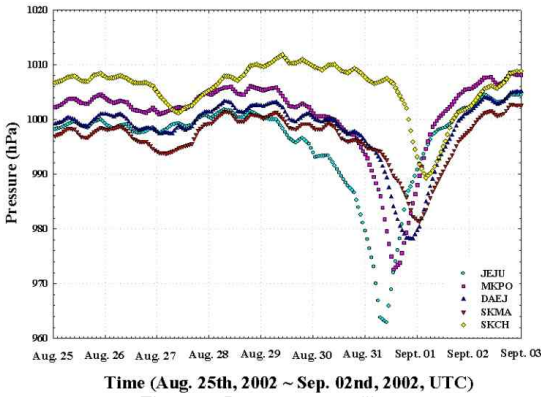

Fig. 7. Pressure profiles
그림 7. 날짜에 따른 GPS관측소 주변의 압력변화도

3-3 PW Comparison between GPS and Radiosonde

Figure 8 shows the PW estimates using GPS and radiosonde measurements, and the pressure profile for station DAEJ, near central part of the Korean Peninsula; Figure 9 SKCH.

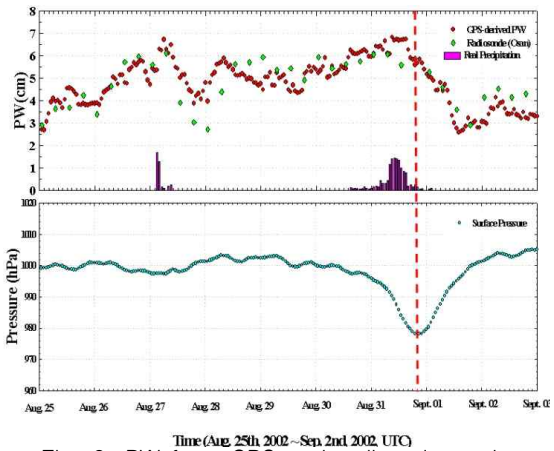

Fig. 8. PW from GPS and radisonde, real precipitation, and pressure profile (DAEJ)
그림 8. GPS, radiosonde로 추정한 가강수량값, 실측강수량 및 압력변화도- 관측소 DAEJ

Both PW estimates generally agreed but there was minor discrepancy due to the different location between the GPS receiver and radiosonde. For station SKCH was the one of the heaviest rainfall stations experienced during the day. It can be validated based on the actual precipitation. The observed PW is high before and during the passage of the typhoon, and then decreased rapidly right after its passage. During the passage of the typhoon, some of the GPS and radiosonde data were missing, indicated by gaps in the plot. The red dashed line represents when the typhoon was close to the station. As seen in the top panel of Figure 9, both PW estimates agreed very well (mostly within 10 mm). Assuming rdiosonde provides true estimates of PW, therefore, the results suggest that GPS could be an excellent alternative of the meteorological device.

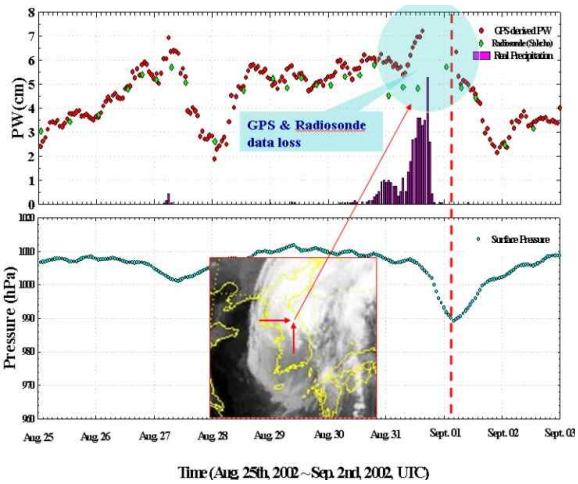

Fig. 9. PW from GPS and radisonde, real precipitation, pressure profile (SKCH)
그림 9. GPS, radiosonde로 추정한 가강수량값, 실측강수량 및 압력변화도- 관측소 SKCH

3-4 ZWD Comparison between GPS and UNB3

ZWD estimates using GPS and UNB3 were also compared at five different sites in Korea during the passage of RUSA. The data processed for this study contained a significant transition of the weather front as indicated in Figure 7. The weather condition during the

first 3-4 days was more or less normal and later it changed to severe weather condition during the passage of the typhoon.

Figure 10 illustrates ZWD estimates at DAEJ station using GPS and UNB3. During the entire period, two ZWD estimates do not agree well. Note that the weather condition was normal for the first 3-4 days. The level of discrepancy in ZWD estimates between GPS and UNB3 is up to 20~30 cm level. This is a substantial difference. If we consider a satellite being tracked at 10-degree elevation, the difference could be easily over 1 m. If mapped to a satellite at 5 degrees, the difference would be over 2 m level. This means that if used, these errors will present in the GPS observations even after applying for the SBAS tropospheric corrections. Consequently, the corresponding navigation solutions could be much degraded.

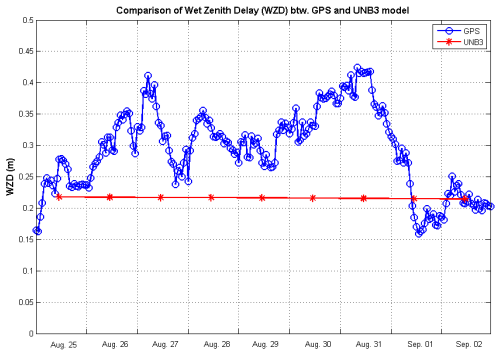

Fig. 10. ZWD from GPS (blue circle) and UNB3 (red star) at DAEJ station
그림 10. 추정된 천정방향 습윤지연비교 – DAEJ

Figure 11 shows the ZWD comparison at JEJU station. During the normal weather condition period before the passage of the typhoon, two approaches generally agreed but not for humid period. The other three stations except JEJU shows similar plot like Fig. 10.

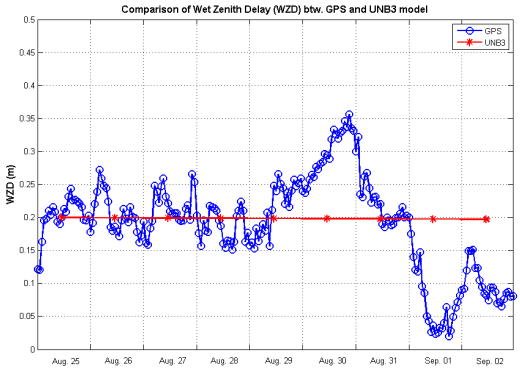

Fig. 11: ZWD from GPS (blue circle) and UNB3 (red star) at JEJU station
그림 11. 추정된 천정방향 습윤지연비교 – JEJU

In general, UNB3 is one of the widely accepted tropospheric mitigation models on GNSS/SBAS community. However, as demonstrated here, there could be many cases which do not improve SBAS positioning solutions. As the lower part of troposphere is highly variable in both time and space, it still remains as an unsolved issue for the high precision GNSS applications.

IV. CONCLUSIONS

For high precision GNSS applications including WA-DGNSS, time-variable tropospheric propagation delay error is one of the limiting factors. Simulation tests were performed in this study to verify if the UNB3 tropospheric delay model can be applicable to WA-DGNSS in the Korea Peninsula. Overall test results indicated the following three important insights about models used:

1) Tropospheric delay estimates using Radiosonde and GPS agreed very well. Assuming radiosonde's estimates are the most accurate, this suggests that GPS can be an excellent weather monitoring tool.

2) Even if the radiosonde provides precise information about the atmosphere, this approach is generally limited by its cost and time. In this case, GNSS or a numerical weather model might be an excellent alternative. As there was no publicly available

numerical weather prediction model in Korea, we tested a ray-tracing based on RUC20 NWP model in Canada, but simulated a humid environment. The results were compared with those of UNB3. The results indicate that the tropospheric delay (mostly slant wet delay) using UNB3 can be much different from that of the RUC20 NWP.

3) During severe weather condition, the tropospheric delay estimates between UNB3 and GPS showed significant difference. This indicates that UNB3 may not be a suitable mitigation method for the troposphere especially in the Korea peninsula.

In conclusion, having a better troposphere mitigation approach is critical for WA-DGNSS. This is because the tropospheric delay is highly correlated with the estimated height component. Once the tropospheric delay is wrongly estimated, the estimated height will not be accurate enough. To have a better approach for the troposphere, further research should be conducted in building a near real-time local troposphere model or an improved version of UNB3 directly applicable to the region.

ACKNOWLEDGEMENTS

This research was supported by a grant from "Development of Wide Area DGNSS" funded by Ministry of Land, Transport and Maritime Affairs of Korean government, contracted through ETRI and Gemini Navsoft Technologies Inc. The authors would like to acknowledge KASI for providing the GPS data sets used for some part of the research reported in this paper.

REFERENCES

[1] Z. Zhu and F. van Graas, “Tropospheric Delay Threats for the Ground Based Augmentation System,” *Proc. ION ITM, San Diego, CA*, 2011.

[2] T. Oguchi, “Electromagnetic Wave Propagation and Scattering in Rain and Other Hydrometeors”, *Proc.oftheIEEE,*Vol.71,No.9.pp.1029-1078,1983.

[3] G. D. Thayer, “An improved equation for the radio refractive index of air”, *Radio Science*, Vol.9, No.10, pp. 803-807, 1974.

[4] T. Schuler, “On Ground-Based GPS Tropospheric Delay Estimation”, *PhDThesis, University of Munchen,* 2001.

[5] U. Hugentobler, S. Schaer, and P. Fridez, “Bernese GPS Software Version 4.2”, *Astronomical Institute, University Berne,* Switzerland, 2001.

[6] V. B. Mendes and R.B. Langley, “Zenith Wet Tropospheric Delay Determination Using Prediction Model: Accuracy Analysis”, *Cartograpiae Cadastro*,Vol.2,pp. 41-47, 1995.

[7] J. Boehm and H. Schuh, “Vienna Mapping Functions”, *16thWorkingMeetingon European VLBI for Geodesy and Astrometry, Leipzig*, pp. 131-143, 2003.

[8] Y. W. Ahn, “Analysis of NGS CORS Network for GPS RTK Performance Using External NOAA Tropospheric Corrections Integrated with a Multiple Reference Station Approach” MScThesis,UCGEReportNumber20211,DepartmentofGeomaticsEngineering,UniversityofCalgary,Canada,2005.

[9] Y. W. Ahn, D. Kim, P. Dare, and R. B. Langley, “Long baseline GPS RTK performance in a marine environment using NWP ray-tracing technique under varying tropospheric conditions”, *Proc. of ION GNSS,* Long Beach, California, U.S.A., pp 2092-2103, 2005.

[10] R. Ghoddousi-Fard, “Modelling Tropospheric Gradients and Parameters from NWP Models: Effects on GPS Estimates”, Ph.D Thesis, Geodesy and Geomatics Engineering, *University of New Brunswick,* 2009.

[11] Moon, Y., “Water Vapor Estimation using GPS Observables”, MScThesis, Department of Astronomyand Space Science, *Yonsei University*, South Korea,1998.

[12] J. Saastamoinen, “Atmospheric correction for troposphere and stratosphere in radio ranging if satellites”, Geophysicalmonograph15,AmericanGeophysicalUnion,*Washington,D.C.*,USA,pp.247-252,1972.

[13] J. L. Davis, T. A. Herring, I. I. Sharpiro, A. E. E. Rogers, and G. Elgerred, “Geodesy by radio interferometry: Effects of atmospheric modeling errors on estimates of baseline length”, *RadioScience,* Vol.20,No.6,pp.1593-1607,1985.

[14] M. Meindl, S. Schaer, U. Hugentobler, and G. Beutler, “Tropospheric gradient estimated at CODE: Results from global solutions”, *Journalof Meteorological Society of Japan*, Vol. 82 (1B), pp. 331-338, 2004.

[15] P. Collins, R. B. Langley, and J. LaMance, “Limiting Factors in Tropospheric Propagation Delay Error Modelling for GPS Airborne Navigation”, TheInstituteofNavigation52ndAnnualMeeting,Cambridge,*Massachusetts,*USA,1996.

[16] W. L. Smith, “Note on the relationship between total precipitable water and surface dew point.” JournalofAppliedMeteorology,Vol.5,October,pp.726-727,1966.

[17] KMA, “Korea Meteorological Administration”, http://www.kma.go.kr/, accessed in 2002.

[18] Y.W., Ahn, D. Kim, and P. Dare, “Positioning Impacts from Imbalanced Atmospheric GPS Network Errors”, *Proc. of ION GNSS, Fort Worth, Texas, U.S.A,* pp. 2302-2312, 2007.

안 용 원 (安勇源)

Mar./1994: BSc, Dept. of Astronomy & Space Science, Chungbuk National Univeristy, South Korea

Jan./2005: MScE, Dept. of Gematics Engineering, University of Calgary, Canada

Feb./2005~cur.: PhD candidate, Dept. of Geodesy and Geomatics Engineering, University of New Brunswick, Canada

Jan./2008~cur.: Instructor, Dept. of Geodesy and Geomatics Engineering, University of New Brunswick, Canada

Interests: GNSS error mitigation, 3D hybrid navigation with scanners, control network surveying, 3D model reconstruction.

김 동 현

Seoul National University: BE (1986), MScE (1993) and PhD (1997)

University of Maine (US): Post-Doctoral fellow (1998)

University of New Brunswick (Canada): Senior Research Associate (2002-2007), Adjunct Professor (2008-present)

Gemini Navsoft Technologies Inc. (Canada): Chief Technical Officer (2008-present)

Dr. Jason Bond

University of New Brunswick (Canada): MScE (2004) and PhD (2007)

Measurand Inc. (Canada): Manager of Engineering (2008-2009)

Gemini Navsoft Technologies Inc. (Canada): Manager of Engineering (2010-present)

최 완 식 (崔完植)

1979년2월: 성균관대학교 기계공학과 (학사)

1986년 8월: The Univ. of Alabama 기계과(공학석사)

1988년8월: The Univ. of Alabama 수학과(응용수학석사)

1992년5월: The Univ. of Alabama, 기계과(공학박사)

1979년3월 – 1984년8월: ADD/국방품질검사소 연구원

1992년6월 - 현재: ETRI 책임연구원

2008년2월 - 현재: TTA LBS 표준화 PG 의장

관심분야: seamless 측위, 위치기반서비스, 최적제어